

The neuronal endopeptidase ECEL1 is associated with a distinct form of recessive distal arthrogryposis

Klaus Dieterich^{1,2,3,4}, Susana Quijano-Roy⁶, Nicole Monnier^{1,5}, Jie Zhou³, Julien Fauré^{1,5}, Daniela Avila Smirnow⁶, Robert Carlier⁷, Cécile Laroche⁸, Pascale Marcorelles⁹, Sandra Mercier¹⁰, André Mégarbané¹¹, Sylvie Odent¹⁰, Norma Romero¹², Damien Sternberg¹³, Isabelle Marty¹, Brigitte Estournet⁶, Pierre-Simon Jouk^{2,3}, Judith Melki⁴ and Joël Lunardi^{1,5,*}

¹Inserm U836, Grenoble Institut des Neurosciences, Equipe Muscle et Pathologie, Grenoble, France ²Département de Génétique et Procréation, ³Centre de Référence des Anomalies du Développement, Hôpital Couple Enfant, CHU Grenoble, Grenoble, France ⁴Institut National de la Santé et de la Recherche Médicale UMR-788, University of Paris 11, Biomedical Institute of Bicêtre, Le Kremlin-Bicêtre 94276, France ⁵Laboratoire de Biochimie Génétique et Moléculaire, Département de Biochimie, Pharmacologie, Toxicologie, CHU de Grenoble, Grenoble, France ⁶AP-HP, Service de Pédiatrie, Hôpital Raymond Poincaré, Garches, Hôpitaux Universitaires Paris-Ile-de-France Ouest, Pôle pédiatrique, Centre de Référence Maladies Neuromusculaires GNMH; CIC-IT—Faculté de Médecine Paris-Ile-de-France Ouest, UVSQ, Versailles, France ⁷AP-HP, Service d'Imagerie Médicale, Hôpital R. Poincaré, Garches, Hôpitaux Universitaires Paris-Ile-de-France Ouest, Pôle neuro-locomoteur, GNMH; UVSQ, Versailles, France ⁸Service de Pédiatrie, CHU Limoges, Limoges, France ⁹Laboratoire d'Anatomo-Pathologie, CHU Brest, Brest, France ¹⁰Service de Génétique Clinique, CHU Rennes, Université Rennes 1, UMR62920, Rennes, France ¹¹Unité de Génétique Médicale et Laboratoire Associé INSERM UMR_S910, Pôle Technologie Santé, Université Saint Joseph, Beyrut, Lebanon ¹²Service d'Anatomopathologie, Pavillon Riessler, Institut de Myologie, Paris, France and ¹³Laboratoire de Cardiogénétique et myogénétique moléculaire et cellulaire, GH Pitié-Salpêtrière, AP-HP, Paris, France

Received November 8, 2012; Revised and Accepted December 2, 2012

Distal arthrogryposis (DA) is a heterogeneous subgroup of arthrogryposis multiplex congenita (AMC), a large family of disorders characterized by multiple congenital joint limitations due to reduced fetal movements. DA is mainly characterized by contractures afflicting especially the distal extremities without overt muscular or neurological signs. Although a limited number of genes mostly implicated in the contractile apparatus have been identified in DA, most patients failed to show mutations in currently known genes. Using a pangenomic approach, we demonstrated linkage of DA to chromosome 2q37 in two consanguineous families and the endothelin-converting enzyme like 1 (ECEL1) gene present in this region was associated with DA. Screening of a panel of 20 families with non-specific DA identified seven homozygous or compound heterozygous mutations of ECEL1 in a total of six families. Mutations resulted mostly in the absence of protein. ECEL1 is a neuronal endopeptidase predominantly expressed in the central nervous system and brain structures during fetal life in mice and human. ECEL1 plays a major role in intramuscular axonal branching of motor neurons in skeletal muscle during embryogenesis. A detailed review of clinical findings of DA patients with ECEL1 mutations revealed a homogeneous and recognizable phenotype characterized by limited knee flexion, flexed third to fifth fingers and severe muscle atrophy predominant on lower limbs and tongue that suggested a common pathogenic mechanism. We described a new and homogenous phenotype of DA associated with ECEL1 that resulted in symptoms involving rather the peripheral than the central nervous system and suggesting a developmental dysfunction.

*To whom correspondence should be addressed: Laboratoire de Biochimie Génétique et Moléculaire, Département de Biochimie, Pharmacologie, Toxicologie, CHU de Grenoble, Grenoble. Tel: +33 476765573; Fax: +33 476765664; Email: jlunardi@chu-grenoble.fr

INTRODUCTION

Arthrogryposis multiplex congenita (AMC) defines congenital joint limitations in at least two different body areas and is a consequence of reduced fetal movement. There are various underlying aetiologies and phenotypic presentations (1).

Distal arthrogryposis (DA) refers to a major subgroup of AMC that is characterized by congenital joint limitations afflicting especially, but not exclusively, the distal extremities without overt muscular or neurological signs. The clinical criteria have been defined to delineate more accurately this subgroup from other types of AMC of neuromuscular origin (2). They include camptodactyly, hypoplastic and/or absent flexion creases, overriding fingers, ulnar deviation of the wrist, talipes equinovarus, calcaneovalgus deformities, vertical talus and/or metatarsus varus. To be considered affected, index cases must exhibit at least two of these major criteria. In clinical practice, DA is not a rare sign in patients attending neuromuscular consultations. This clinical entity encompasses well-characterized DA, but also all congenital joint limitations that fulfil the major clinical criteria but fail to overlap with one of the well-defined DA types (3). To date, the genetic background has been characterized only in a minority of DA, affecting almost exclusively genes encoding proteins associated with the contractile apparatus of the skeletal muscle: *MYH2*, *MYH3*, *MYH8*, *MYBPC1*, *TPM2*, *TPM3*, *TNNI2*, *TNNT3*, *ACTA1*, *NEB* genes (4–11) or the skeletal muscle calcium homeostasis: *RYR1* (12).

AMC has also been reported in disorders of the neuromuscular junction. Fetuses born to mothers producing antibodies directed against the fetal form of the acetylcholine receptor (AChR) were shown to develop AMC (13) and mutations of the genes encoding subunits of the AChR have been reported to cause AMC (14–17). AMC have also been associated with mutations in the *RAPSN* and *DOK7* genes that encode proteins involved in the AChR clustering at the post-synaptic membrane (16,18). AChR deficiency at the neuromuscular junction appears, therefore, as a common pathway to AMC in autoimmune or genetically related myasthenic syndromes (19). However in most DA, no molecular cause has been yet identified and genetic counselling relies only on empirical evaluation and precludes early prenatal diagnosis.

A genome-wide single-nucleotide polymorphism (SNP) genotyping approach allowed mapping of a disease locus genetically associated with DA to chromosome 2q36.3–2q37.3 in two consanguineous families of different geographical origin. This allowed the characterization of a novel gene, endothelin-converting enzyme like 1 (*ECEL1*), previously known to be involved in the development of neuromuscular junctions (20,21). *ECEL1* mutations were identified in six families with very similar clinical features and muscle magnetic resonance imaging (MRI) involvement making the *ECEL1* gene a frequent cause of autosomal recessive DA.

RESULTS

Mapping of the disease locus on chr 2q37

Homozygosity mapping performed in consanguineous family F1 (Fig. 1) defined 10 homozygous regions with a size ranging

from 0.3 Mb to 8.3 Mb present only in the three affected children (Supplementary Material, Fig. S1) and pointed towards a locus on Chr. 2q37 with a maximum LOD score $Z_{\max} = 3.1$ at $\theta = 0.0$. A second genome-wide SNP genotyping performed in the consanguineous family F5 (Fig. 1) helped to reduce the size of the disease locus to 5.17 Mb. The recombinant events were observed between rs2396608 and rs6708323 (Chr. 2: 229933418–235110179, NCBI human genome build 37.3). Combining multipoint linkage data from the two multiplex families confirmed the locus on Chr. 2q37 with a maximum LOD score $Z_{\max} = 5.1$ at $\theta = 0.0$ (Fig. 2). As presented in Figure 2 and listed in Supplementary Material, Table S1, this interval contained 77 annotated genes (NCBI human genome build 37.3) including the *CHRNA* and *CHRND* genes known to cause arthrogryposis-associated congenital myasthenic syndromes (14–17). Sanger sequencing excluded pathological sequence variants in both genes for the two families F1 and F5. We then looked for candidate genes expressed in muscle, nerve or at the neuromuscular junction as highlighted by the relevant literature and by the GeneHub-GEPIS database (22). The *ECEL1* gene appeared as a potential target gene because of its essential function in mice for the formation of neuromuscular junctions during the developmental stages of the central and peripheral nervous system (PNS) (23,24).

ECEL1 mutations are associated with recessive forms of DA

Sequencing of the *ECEL1* gene with specific primers (Supplementary Material, Table S2) in our panel of 20 families with DA evidenced seven variants in a total of six families (Fig. 1). A homozygous c.[1649C>G]+[1649C>G], p.[Ser550*]+[Ser550*] non-sense mutation was identified in the two affected children of consanguineous family F2, whereas compound c.[1470G>A]+[997C>T], p.[Try490*]+[Arg333*] heterozygous non-sense mutations were identified in affected proband II:1 of family F3. A homozygous c.[874delG]+[874delG] frame shift mutation generating a premature termination of the protein, p.[Val292Cysfs*51]+[Val292Cysfs*51], was evidenced in consanguineous family F4.

Two distinct homozygous mutations, c.[1685+1G>T]+[1685+1G>T] and c.[966+1G>A]+[966+1G>A] that affected consensus acceptor splice sites of introns 10 and 4 were identified, respectively, in families F5 and F6. Both the mutations were defined as pathogenic using the Human Splicing Finder predictive software (<http://www.umd.be/HSF/HSF.html>). The c. [1685+1G>T] mutation generated two abnormal transcripts that introduced premature termination codons (p.Lys552AlafsX33 and p.Asp559AlafsX33) (Supplementary Material, Fig. S2). No muscle tissue was available for patient II:2 in family F6 to study the consequences of the c.[966+1G>A] mutation. Non-sense, frame-shift and splice mutations would thus either yield a truncated protein devoid of its catalytic domain (Fig. 3A) and/or lead to a non-sense-mediated mRNA decay, suggesting in all situations a loss of function for *ECEL1*.

A c.2278C>T transition in exon 18, leading to a cysteine to arginine substitution at position 760 (p.Cys760Arg) of the protein, was identified in family 1. As shown in Figure 1, the mutation was present at a homozygous level in the three

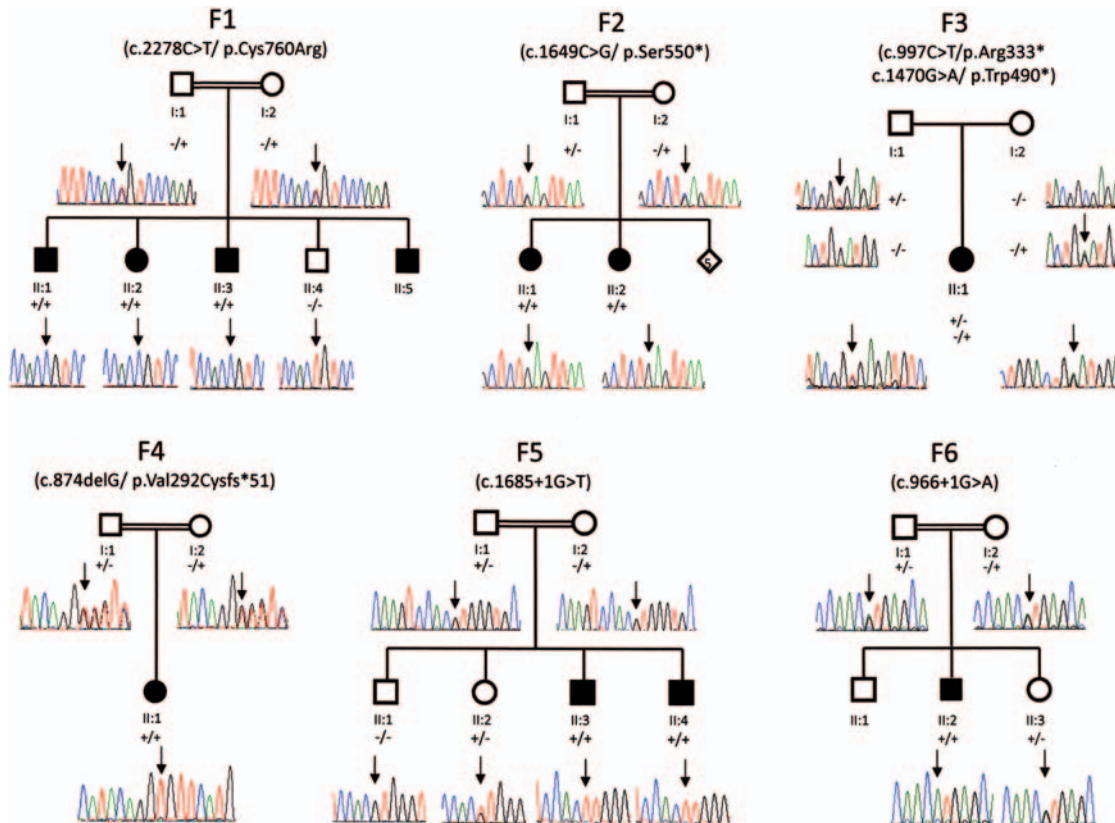


Figure 1. Pedigrees of DA families with ECEL1 mutations. Electropherograms from direct ECEL1 sequencing of the affected individuals and their available relatives are presented below individuals. # symbols indicate individuals that were genotyped using the 250 K Nsp arrays. Arrows indicate mutant or wild-type nucleotide position. Open symbols = unaffected; filled symbols = affected; squares = male; circles = female; plus = mutant allele; minus = wild-type allele. Individuals without electropherograms were not analysed.

affected patients. No DNA was available for patient II:5. The p.Cys760Arg was linked to the disease with a highly significant LOD score of 3.1, and it was not found in 100 chromosomes from geographically matched individuals and affected a highly conserved cysteine (Fig. 3B). Predictive softwares classified the p.Cys760Arg variant as pathogenic [Polyphen-2 (<http://genetics.bwh.harvard.edu/pph2/>), SNPs&GO (<http://snps-and-go.biocomput.unibo.it/snps-and-go/>), MutPred (<http://mutpred.mutdb.org/>)]. Cysteine 760 is one of the 10 phylogenetically highly conserved cysteine residues throughout the NEP enzyme family (Fig 2B) (25). The cysteine 760 was implicated into the formation of a disulfide bond with cysteine residue 772 that is involved in the catalytically active consensus site of ECEL1 (25–27). Unlike other endopeptidases of the NEP family, ECEL1 is predominantly expressed into the endoplasmic reticulum (28). As the p.Cys760Arg mutation did not alter the targeting of ECEL1 (Supplementary Material, Fig. S3), the pathogenic effect of the mutation is likely to be associated with an alteration of the catalytic site.

ECEL1 mutations are associated with a typical phenotype

Prenatal findings associated with arthrogryposis in our patients were limited to diminished fetal movements (patients F2/II:2, F3/II:1) and persistent knee extension on ultrasound examination during the third trimester (family F1). These findings

are not specific and ultrasound examinations were otherwise normal when performed (families F3, F4 and F5). An intra-uterine growth retardation was present at birth in three patients (F3/II:1, F5/II:3, II:4), yet its link to the DA phenotype and ECEL1 is not clear. Delivery was at term for patients F2/II:1, II:2; F3/II:1; F4/II:1; F5/II:3, II:4 with a breech presentation reported for patients F2/II:1 and F3/II:1. None of the patients had a history of respiratory distress during the neonatal period.

As presented in Table 1 and Figure 4, all patients showed DA with flexion contractures of fingers III–V, limited knee flexion, and talus, talus valgus or varus deformity of feet (Fig. 4A–D). Lower limbs were more extensively affected than upper limbs. Absence or limited knee flexion was not associated with lack of patella. All cases but one had hip involvement consisting in congenital hip dislocation or limited mobility. In contrast, none of the cases had major elbow or shoulder girdle contractures. Noticeably no pterygia were found. Other frequent findings observed in the series were short neck and muscle atrophy, predominant in lower limbs. Three patients had a hyperlaxity of distal joints in addition to distal joint contractures. Osteotendinous reflexes were often found abolished in very severely amyotrophied regions, but present in those with only moderate muscle atrophy. Two frequent and striking features were a spared or less involved index finger (Fig. 4F–I) and a central tongue atrophy leading to a grooved shape (Fig. 4K–N).

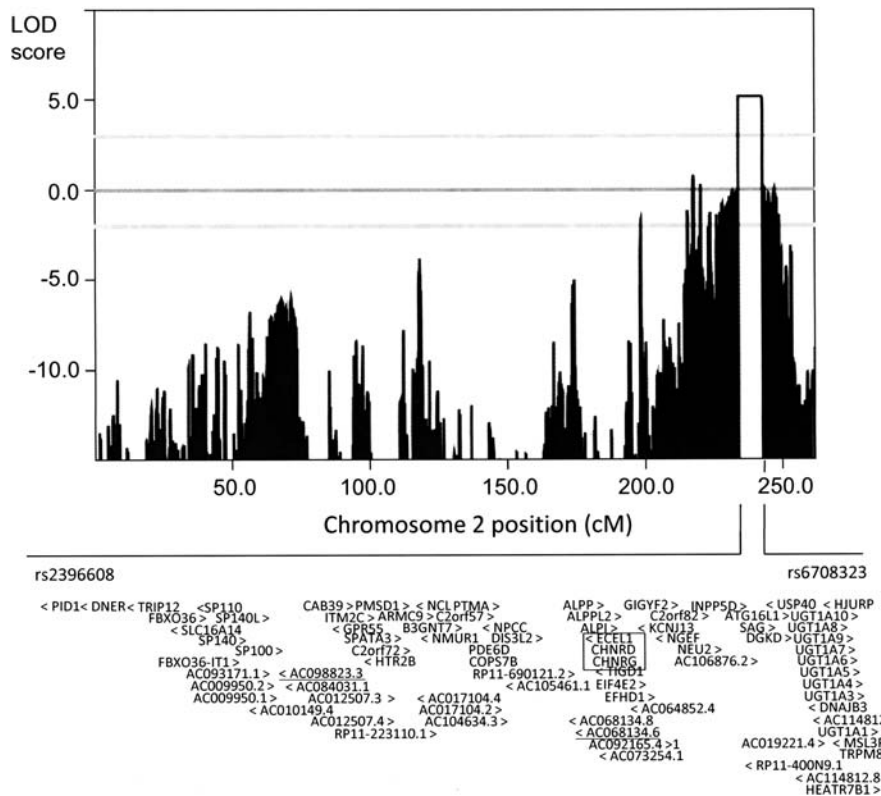


Figure 2. Linkage and homozygosity mapping analysis of families F1 and F5. Combined results of linkage analysis showing a maximum LOD score $Z_{\max} = 5.1$ at $\theta = 0.0$. X-axis: genetic distance in cM., Y-axis: Lod score. Data obtained for patients I:1, I:2, II:1, II:2, II:3, II:4 of family 1 and patients I:1, I:2, II:1, II:2, II:3, II:4 of family 5 were used. The lower part of the panel indicates the annotated sequences present in the interval spanning between rs2396608 and rs6708323. A more detailed list of the candidate genes present in this region is presented in Supplementary Material, Table S1.

Mild-to-severe scoliosis (Fig. 4E) was a frequent complication. In family F1, the three siblings developed early progressive deformities that required a very close orthopaedic treatment by rigid Garches brace and trunk night casts during childhood. Arthrodesis was performed in two patients (F2/II:2; F3/II:1). A restrictive pulmonary insufficiency was detected in four patients (F1/II:1, II:2, II:3; F3/II:1), but none required mechanical ventilation. Joint limitations were stable or improved on physiotherapy. All patients achieved independent walking between 18 months and 3 years of age. Fatigability was reported but muscle strength was relatively stable, except in one patient (II:4 in family F5) who experienced progressive loss of muscle force during childhood and was forced to use a manual wheel chair for outdoor activities from the age of 10.

Ptosis was noted for a majority of patients. In addition to ptosis, ocular clinical findings in patients with ECEL1 mutations included lagophthalmos and pseudo-exophthalmos features (Supplementary Fig. S4A,B) and Duane syndrome in patient F1/II:3 (Supplementary Material, Fig. S4C,D). Except for a patient who had Duane syndrome of the left eye, oculomotricity was normal. No sensory symptoms were found. Although no formal testing was done, no cognitive impairment was noted and all children had a normal-to-age school level. Half of the patients complained of mild speech difficulties that could result from the grooved shape of the tongue. Sucking or swallowing difficulties were only noted in one patient (Table 1 and Supplementary Material, Table S3).

Paraclinical findings

T1-weighted whole body, or lower extremities muscle MRI views were obtained for six patients. All showed a severe fatty muscle replacement (porcelain-like infiltration) that affected mainly the thigh as shown in Figure 5 and that was evaluated by use of the Mercuri score (29) (Supplementary Material, Fig. S5). The biceps femoris (BF), sartorius and partially the vastus lateralis muscles were selectively affected, while rectus femoris (RF) and gracilis (G) were systematically spared. Fatty replacement in distal leg muscles was also frequent and the particularity at this level was a diffuse and often asymmetric involvement. Frontal views in four patients showed a thoracic spinal deformity associated with paravertebral muscle hyperintensity, while neck and upper limb muscles were spared (Fig. 3, E). In the head, the most striking finding was a severe central atrophy of the tongue leading to a bifid shape (Fig. 4, O).

Four mutated patients had muscle biopsies. As presented in Supplementary Material, Figure S6, neither major structural abnormalities of the sarcolemma nor any signs reminiscent of denervation were observed in any of the muscle biopsies studied. Nonetheless, type 1 fibre type predominance (F1/II:1 and 2, F3/II:1) (A, D, G); mild difference in the fibre size (F1/II:1 and 2) (B, E, H) and moderate lipid storage (F1/II:1 and 2, F5/II:3) (F, F, I) were observed in biopsies.

Electrophysiological testing was performed in eight patients harbouring ECEL1 mutations. Five showed normal results

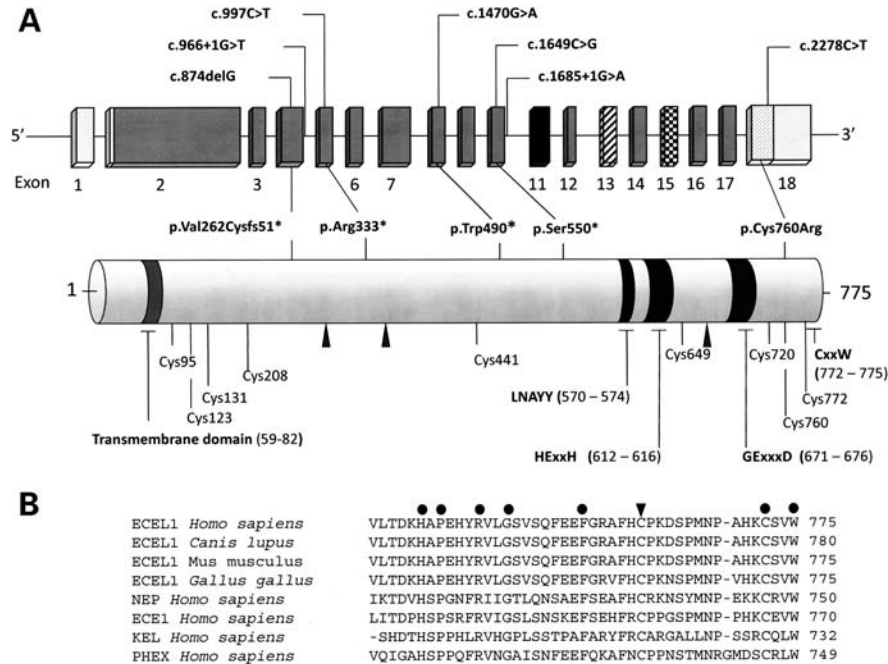


Figure 3. ECEL1 mutations identified in the patients with DA. (A) Mutations indicated as nucleotide changes are presented in the upper part of the panel, while consequences of mutations at the protein level are indicated in the lower part of the panel. Upper part: the blackened exon 11 contains the LNAYY motif involved in substrate orientation; the hatched exon 13 contains the HExxH zinc binding motif,²⁰ the checked exon 15 contains the GExxxD zinc coordinating motif^{20,33} and the dotted exon 18 contains the CxxW metalloprotease conserved carboxy terminal sequence.³⁵ Light grey regions correspond, respectively, to the 5' and 3' untranslated sequences. Lower part: phylogenetically conserved cysteinyl residues involved in the formation of disulphide bridges are indicated. LNAYY: motive important for the orientation of the substrate peptide bond to be cleaved. HExxH: zinc binding motive. GExxxD: zinc coordinating motive. CxxW: metalloprotease conserved carboxy terminal sequence. Arrows: putative N-glycosylation sites (20, 25, 34). (B) Alignment of protein sequences from human ECEL1 (NP_004817.2), ECEL1 orthologues (dog ECEL1, XP_543287.2; mouse ECEL1, NP_067281.2; chicken ECEL1, XP_422744.3 and members of the human M13 endopeptidase family such as neprolysin (NEP, NP_009220.2), endothelin-converting enzyme type I (ECE1, NP_001388.1), Kell blood group metalloendopeptidase (KEL, NP_000411.1) and phosphate-regulating endopeptidase homologue X-linked (PHEX, NP_000435.3). Arrow points to the conserved cysteine residue at position 760 of human ECEL1 that is mutated in family 1. Dots indicate other conserved amino acids in the C-terminal domain of ECEL1.

with electromyography (EMG) and nerve conduction velocity measurements performed at ages ranging from 8–11 years (Supplementary Material, Table S1). In two patients (F2/II:2, F5/II:3), the needle EMG was suggestive of myopathy at the 13th day after birth and 2 years of age, respectively. One patient (F3/II:1) had repeated studies. The first was done at age 3.5 years and included motor and sensory nerve conduction studies (NCSs) only of lower limbs and needle EMG only in proximal muscles of the lower and upper extremities. It was reported as normal. The second study was performed at 18 years. It included distal muscles investigation and revealed neurogenic signs (Supplementary Material, Fig. S7 and Table S3).

Additional clinical and biochemical analyses performed to exclude neuromuscular, cardiac or ophthalmologic abnormalities yielded normal results. Serum CPK levels were found within the physiological limits in patients from two different families (Supplementary Material, Table S3).

DISCUSSION

This study provides molecular and clinical evidence that mutations of ECEL1, a neuronal endopeptidase not yet associated with pathologies in humans, caused a hitherto not recognized

DA that differed from other formerly described types of DA by its autosomal recessive inheritance and its recognizable clinical features.

A review of clinical findings in our panel of patients harbouring mutations in the *ECEL1* gene revealed a number of distinct features including limited knee flexion, absent or only mild flexion contractures of the index fingers, tongue atrophy and scoliosis (Table 1, Fig. 4). Tongue atrophy is usually reported in patients with autoimmune myasthenia (30) and more occasionally in patients with congenital myasthenic syndromes (CMS). However, myasthenic patients present other signs not observed in our patients, such as bulbar weakness and striking fatigue with repetitive movements leading to variable motor function in the course of the day.

Muscle biopsies were normal or showed mild non-specific abnormalities. No neuropathic or major structural muscular abnormalities were found, however, it must be noted that only proximal muscles were studied (deltoid and quadriceps). The increased content of lipids detected in the muscle fibres could contribute to the abnormal hyperintensity evidenced by muscle MRI.

When performed NCSs were normal. This finding allowed us to rule out a sensorimotor polyneuropathy. When specifically studied, repetitive stimulation and stimulated single-fibre electromyography failed to demonstrate a dysfunction of the

Table 1. Clinical findings: most frequent clinical findings in ECEL1 mutated patients were flexed III–V fingers (10/10) with a spared or less involved index finger (8/9), limited knee flexion (10/10), talus or talus valgus feet deformity (9/10), diminished muscle mass (10/10), short neck (10/10), tongue atrophy (7/7) and bilateral or unilateral ptosis (7/10).

	Family 1 Mali			Family 2 Belgium		Family 3 Martinique	Family 4 Turkey	Family 5 Morocco		Family 6 Lebanon	Total
	II:1	II:2	II:3	II:1	II:2	II:1	II:1	II:3	II:4	II:1	
Date of birth	2001	2002	2003	1971	1980	1993	2009	1999	2003	1997	
Face											
Ptosis	+	–	– ^a	+	+	–	+	+	+	+	7/10
Abnormal oculomotricity	–	–	– ^a	–	–	–	–	–	–	–	1/10
Pseudo-exophthalmos and lagophthalmos	–	–	–	+	+	–	–	–	–	–	2/10
Decreased facial movements	–	–	+	+	+	–	–	?	?	?	3/7
Mouth held open	–	–	+	+	–	–	–	–	+	+	5/10
Small mouth	–	–	–	+	–	–	+	–	+	–	3/10
Tongue atrophy	+	+	+	+	+	+	?	?	?	+	7/7
Speech difficulties	?	+	+	+	+	?	NA	?	?	+	5/5
Short neck	+	+	+	+	+	+	+	+	+	+	10/10
Upper limbs											
Limited shoulder movement	–	+	+	–	–	–	?	–	–	?	2/8
Limited elbow movement	+	–	–	–	–	+	?	+	?	?	3/7
Flexed fingers III–V	+	+	+	+	+	+	+	+	+	+	10/10
Spared or less involved index finger	+	+	+	+	+	–	+	+	+	?	8/9
Distal interphalangeal joint hyperlaxity	–	–	–	+	?	+	–	+	+	?	4/8
Vertebral column											
Scoliosis	+	+	+	+	+	+	– ^b	–	–	+	7/10
Hyperlordosis	+	+	+	+	+	+	?	+	+	+	9/9
Lower limbs											
Congenital hip dislocation and/or limited hip movement	+	+	+	+	+	+	+	+	+	?	9/9
Limited knee flexion	+	+	+	+	+	+	+	+	+	+	10/10
Talus or talus valgus deformity of feet	+	+	+	+	+	+	– ^c	+	+	+	9/10
Diminished muscle mass (predominantly on lower extremities)	+	+	+	+	+	+	+	+	+	+	10/10
Osteotendinous reflexes	+	?	?	+	+	?	–	+	+	–	5/7
Sucking and swallowing difficulties	–	–	–	–	–	–	–	–	–	+	1/10
Pyramidal signs	–	–	–	–	–	–	–	–	–	–	0/10
Sensitive signs	–	–	–	–	–	–	–	–	–	–	0/10

^aDuane syndrome type 1 of the left eye; NA—not applicable; ^bat 18 months of age; ^cvarus deformity; ?, not reported.

neuromuscular junction transmission. However, investigations were only performed in one patient and will require confirmation. Needle EMG was abnormal in three children, evoking a myopathy in two infants, but revealing chronic neurogenic abnormalities in muscles of hands and feet in an 18-year-old girl. Extensive investigations are clearly needed in patients with ECEL1 mutations to investigate a potential pathogenic process affecting the nerves or the lower motor neurons.

The homogeneity of the clinical phenotype regardless of the type of mutation identified in patients suggested a common underlying mechanism. In five out of six families (F2, F3, F4, F5, F6), mutations of the *ECEL1* gene generated premature stop codons that mapped upstream the different motives associated with the peptidase activity of ECEL1 (20,31). As presented in Figure 3, these mutations if expressed would yield a truncated protein devoid of its catalytic domain. Furthermore and as illustrated in Supplementary Material, Figure S2, premature stop codons could lead to a non-sense-mediated mRNA decay process (32). In both situations, the expected effect of the mutations would be an absence of synthesis of functional ECEL1. The p.Cys760Arg missense mutation affected a well-conserved amino acid and introduced a significant chemical change with a Grantham score of 180 (33) in a region that is critical for protein maturation and enzyme activity. Genetic criteria, including lod score analysis and predictive softwares, defined

this mutation as pathogenic. The high conservation of the terminal cysteine residues in the NEP family and their structural role in protein folding suggested that cysteine 760 of ECEL1 is critical for proper maturation and folding of the enzyme (25,26,34–37). Based on these different data the pathogenic effect of the p.Cys760Arg mutation would thus result from the loss of the catalytic activity as a consequence of an alteration of the folding of the carboxy terminal catalytic region. Absence of knowledge regarding the physiological peptidic substrate of ECEL1 prevented further testing of the effect of the mutation on the specific physiological function.

The pathogenic mechanism of this novel type of DA caused by mutation of ECEL1 is still poorly understood. ECEL1, alternatively called damage-induced neuronal endopeptidase, is a neuron-specific endopeptidase belonging to the neutral endopeptidase (nepilysine, NEP) family (20,21,23). ECEL1 is expressed from early developmental stages in both the central and the PNS (21,23) and appeared to have a non-redundant and essential function in rodents (24,38). ECEL1-deficient mice die from respiratory dysfunction shortly after birth as a consequence of embryonic developmental defect of final axon branching of motor neurons in skeletal muscle that led to a significant reduction of neuromuscular junctions (21,38,39). Nonetheless, the overall ultra-structure of the presynaptic terminal, the terminal Schwann, the muscle cell and initial AchR

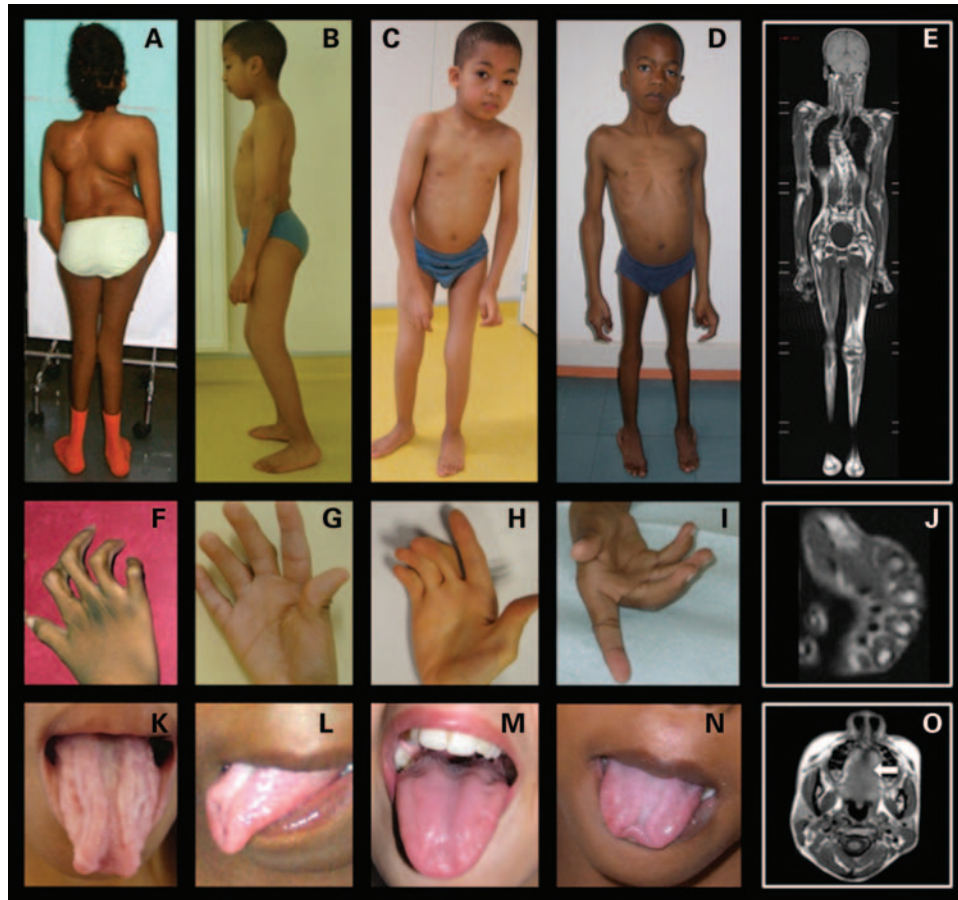


Figure 4. Clinical phenotypes of patients harbouring *ECEL1* mutations. (A–D) Global phenotypic appearance is marked by muscle atrophy especially in the lower extremities, hyperlordosis with limited hip extension, fixed slightly flexed knees with limited active knee flexion, pes valgus and finger flexions. (A) individual F3/II:1; (B) individual F5/II:3; (C) individual F5/II:4; (D) individual F1/II:1. (F–I) Clinical findings on hand examination were particular in that index fingers were almost constantly spared or less involved than fingers III–V, showing normal or less hypoplastic flexion creases. Hallux hyperextensibility was a common feature. (F) Individual F3/II:1; (G) individual F5/II:4; H: individual F2/II:1; (I) individual F1/II:1. (K–N). Tongue atrophy presenting as a deep groove in the middle of the tongue was a constant feature when searched for, sometimes also involving the tip of the tongue. (K) individual F3/II:1; (L) individual F1/II:2; (M) individual F6/II:1; N: individual F1/II:1. (E, J, O): WB-MRI T1 TSE sequences of patient II :1 from family I presented in adjacent panels D, I, N. The frontal whole-body view (E) shows thoracic scoliosis and relative preservation of neck and upper limb muscles. The axial views (J and O) show the striking preservation of muscle signals in hand (panel J), neck and masticator muscles (panel O), while the tongue tip is bifid due to central atrophy (arrow in O).

clustering remained unaffected in mice. In rodents, *ECEL1* is specifically expressed in neuronal tissues (21). At difference with this situation, additional expression of *ECEL1* was also detected in skeletal muscle and pancreas in human (20). As shown in Supplementary Material, Figure S8, *ECEL1* was expressed during embryogenesis in humans both in CNS structure like spinal cord and in skeletal muscle. The differential pattern of expression of *ECEL1* in humans and rodents could be part of the explanation of the different phenotype presented at birth by *ECEL1*-deficient mice and patients homozygous for mutations affecting *ECEL1* synthesis. Such a situation is comparable with that observed for arthrogryposis syndromes caused by mutations of the *CHNRG* gene. *CHNRG*-deficient mice died shortly after birth from respiratory failure, whereas *CHNRG* mutated patients showed a viable and non-progressive AMC without respiratory symptoms in the neonatal period (14,15). A proposed explanation for this difference was the different switching between the fetal and adult forms of AchR in humans and mice (40,41). However, no developmentally

expressed isoforms of *ECEL1* have been yet identified and the three known pseudogenes of *ECEL1* are non-coding (42). An alternative explanation would be the presence in humans of a redundant or compensatory mechanism for *ECEL1* function in axon branching that will take place after the critical time interval for intramuscular motor neuron branching.

Children had a normal-to-age school level and whole-body MRI examinations produced normal brain images. Clinical examination revealed mild muscle weakness (all patients were ambulatory), more predominant in distal limbs, reduced or absent osteoarticular reflexes and hypotonia. However besides these signs, no other major central nervous system involvement was evidenced in our patients. Several children developed a severely progressive scoliosis and a restrictive respiratory insufficiency, both complications frequently observed in the course of early-onset neuromuscular disorders. Weakness seemed to be stable during the time and joint contractures were unchanged or improved after birth, thus suggesting rather a developmental than a degenerative disorder of the PNS.

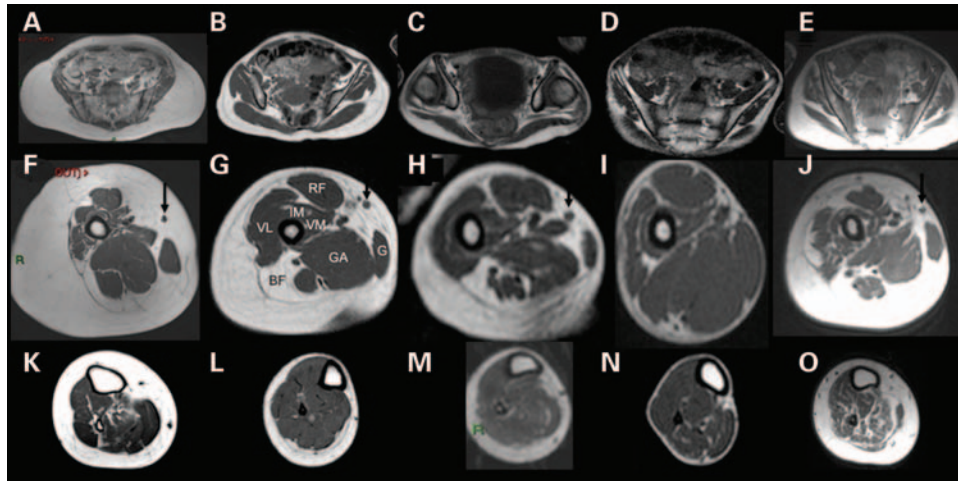


Figure 5. Muscle MRI findings in patients harbouring *ECEL1* mutations. Pelvic girdle and lower limb muscle MRI in T1-TSE sequences. A homogeneous pattern of muscle involvement with a “porcelain-like” abnormal signal is shown in the muscles of five cases of the series (patient F2/II:2 = A, F, K; patient F3/II:1 = B, G, L; patient F1/II 2:1 = C, H, M; patient F1/II :2 = D, I, N; patient F1/II-3 = E, J, O). At the pelvic girdle (A–E), there was poor muscle bulk of gluteus maximus and a thick hyperintense signal between maximus and medius gluteus. In the thigh (F–J), there was a striking hypertrophy of the RF, great adductor and gracilis (G) muscles, while sartorius muscle was severely atrophic (arrows). Thick “porcelain-like” hypersignal lesions were observed in other muscles including vastus lateralis, intermedius and medialis (VL-IM-VM), BF. At the lower leg level (K–O), patterns were less clear with normal findings (L and M), mild soleus changes (K and N) and diffuse atrophy and infiltration predominant in the posterior compartment (O).

The fatty replacement of muscle evidenced by muscle MRI suggested a predominant PNS disease (Fig. 5). Moreover, there was a homogeneous and recognizable pattern of involvement observed in all the patients, in particular in lower limbs, often asymmetric and with the BF muscles being always severely affected (Supplementary Material, Fig. S5). However, the origin of these signal abnormalities cannot be determined by MRI and the review of additional studies of the PNS was not yet conclusive.

In conclusion, we showed that the *ECEL1* gene is a gene frequently associated with a clinically recognizable autosomal recessive form of DA with antenatal presentation that is likely to reflect a novel pathogenic mechanism. Patients will greatly benefit from the investigations of the *ECEL1* gene for clinical diagnosis and genetic counselling. No dysfunction of the neuromuscular transmission was evidenced and motor neuron involvement is rather suspected on the basis of preliminary electrophysiological results, although direct evidence are still incomplete. Further studies in patients and investigations of the neuromuscular junction formation in muscles of patients affected by DA linked to *ECEL1* mutations together with the characterization of the physiological substrate of *ECEL1* will help us in elucidating the pathogenic mechanism leading to this form of DA.

SUBJECTS AND METHODS

Patients and DNA samples

This study was approved by the Ethical Committee of the Grenoble University Hospital (Comité de Protection des Personnes Sud-Est, France) and all family members provided written informed consent prior to genetic analysis.

The panel of 20 families included in the study presented with congenital arthrogyposis associated with distal involvement as a

prominent feature, non-progressive course of the disease and without any other organ or cognitive involvement. An autosomal recessive inheritance was suggested in five consanguineous families and in one non-consanguineous family with two affected children. All other cases were sporadic.

DNA was extracted from whole blood according to the standard protocols. The quantity and quality of DNA were determined on a NanoDrop ND-2000C UV-Vis spectrophotometer (Nanodrop Technologies, Wilmington, DE).

Genome-wide SNP genotyping and homozygosity mapping

DNA samples from 5 affected patients and 7 unaffected individuals (Fig. 1) of two consanguineous families of Malian (Family F1) or Moroccan origin (Family F5) were genotyped for 264 422 SNPs using the Genechip Human Mapping Affymetrix® 250 K Nsp arrays (Affymetrix, Santa Clara, CA, USA) according to the manufacturer’s instructions. Multipoint linkage analysis and homozygosity mapping of SNP data were performed using the Alohomora (43) and Merlin (44) softwares with the following parameters: autosomal recessive inheritance, 100% penetrance and a theoretical disease gene frequency in the population of 1 : 1000.

Analysis and characterization of *ECEL1* mutations

Coding exons and splice junctions of the *ECEL1* gene were analyzed by bidirectional Sanger sequencing of proband’s DNAs using an ABI 3130 XL DNA analyser (Life Technologies, Carlsbad, CA, USA). Primers were designed to span the coding exons and splice junctions of the *ECEL1* gene using the Primer3 program (www.frodo.wi.mit.edu) and the NCBI genomic reference sequence (NM_004826.2). DNA sequences harbouring mutations were subsequently analysed in relatives to confirm familial segregation. None of the identified *ECEL1*

variants have been detected in 200 chromosomes of the general population. When needed total RNAs were extracted from the frozen muscle specimen by using Trizol (Invitrogen, Carlsbad, CA, USA) and complementary DNA (cDNA) was synthesized using the Transcriptor System (Roche, Basel, Switzerland).

ECEL1 mRNA expression pattern in fetal and adult tissues

Lymphoblastoid cell lines were derived from healthy control individuals. Tissues were collected from aborted fetus at 12 weeks of gestation for disease unrelated to neuromuscular defect in the framework of prenatal diagnosis and with the informed consent of parents. Adult skeletal muscle was collected in the frame of muscle biopsy for a disease unrelated to arthrogryposis and following the informed consent of patient. Total RNAs were extracted by using the TRI Reagent LS method (Sigma-Aldrich, Saint Louis, MO, USA) and cDNA was synthesized using the SuperScript[®] III reverse Transcriptor system (Invitrogen).

MRI imaging

Four patients (F1/II:1, II:2, II:3; F3/II:1) underwent whole-body muscle MRI (WB-MRI) examinations using a 1.5-Tesla Philips MRI system (Achieva Release 11, Philips Medical Systems, Eindhoven, The Netherlands), with a previously described protocol that includes T1-weighted turbo spin echo (T1-TSE) and STIR sequences (45). This technology allowed frontal and axial views. Two adult patients underwent sequential MRI examinations that only allowed axial views, exploring upper and lower limbs (F2/II:1) or only lower limbs (F2/II:2).

Immunohistochemical and electronic microscopy muscle imaging

Skeletal muscle biopsies were analysed in four patients (deltoid muscle for F1/II:1, II:2 and F5/II:1; quadriceps muscle for F3/II:1) (Supplementary Material, Fig. S6). Parts of each muscle biopsy were frozen immediately in isopentane cooled in liquid nitrogen and stored at -80°C until processing. Histo-enzymological studies were carried out on 10 mm transverse cryostat sections according to the protocols described previously (12,46).

Neuromuscular electrophysiological studies

Motor and sensory NCSs were performed using the standard procedures and a Medtronic portable Keypoint EMG system (Medtronic, Minneapolis, MN, USA). In order to search specifically for abnormalities in nerve, muscle or neuromuscular junction, a prospective study including SSFEMG (46,47) was performed by S.Q.R. in patient F3/II:1 after obtaining signed consent (Supplementary Material, Fig. S7).

SUPPLEMENTARY MATERIAL

Supplementary Material is available at *HMG* online.

ACKNOWLEDGEMENTS

We are indebted to all patients and family members who participated in this study. Special thanks go also to the laboratory members who participated in cell expression studies (Isabelle Durieux, Marine Cacheux; Grenoble Institut des Neurosciences, Grenoble, France), in sequencing studies (Nadine Teissier, Marina Lamaria, Séverine Drouin; laboratoire de Biochimie et Génétique Moléculaire, CHU de Grenoble, France), in histological and ultra-structural analyses (Emmanuelle Lacène; Pavillon Rissler, Groupe Hospitalier Pitié-Salpêtrière, Paris, France) and in contact with the families (Dr Danielle Leclair-Richard, Hôpital de Garches, Hélène Rauscent, CHU de Rennes).

Conflict of Interest statement. None declared

FUNDING

D.K. was granted a scholarship from the Fédération pour la Recherche Médicale and was supported by a local research grant of the Direction pour la Recherche Clinique et de l'Innovation of the CHU de Grenoble and of the Bicêtre University Hospital. This work was supported by grants from ANR-Maladies Rares, Association Française contre les Myopathies (AFM), the Programme Hospitalier de Recherche Clinique (AOM 10181) and Inserm (to J.M.).

REFERENCES

- Hall, J.G. (1997) Arthrogryposis multiplex congenita: etiology, genetics, classification, diagnostic approach, and general aspects. *J. Pediatr. Orthop. B*, **6**, 159–166.
- Bamshad, M., Jorde, L.B. and Carey, J.C. (1996) A revised and extended classification of the distal arthrogryposes. *Am. J. Med. Genet.*, **65**, 277–281.
- Bamshad, M., Van Heest, A.E. and Pleasure, D. (2009) Arthrogryposis: a review and update. *J. Bone Joint Surg.*, **91**(Suppl 4), 40–46.
- Oldfors, A. (2007) Hereditary myosin myopathies. *Neuromuscul. Disord.*, **17**, 355–367.
- Toydemir, R.M., Rutherford, A., Whitby, F.G., Jorde, L.B., Carey, J.C. and Bamshad, M.J. (2006) Mutations in embryonic myosin heavy chain (MYH3) cause Freeman–Sheldon syndrome and Sheldon–Hall syndrome. *Nat. Genet.*, **38**, 561–565.
- Gurnett, C.A., Desruisseau, D.M., McCall, K., Choi, R., Meyer, Z.I., Talerico, M., Miller, S.E., Ju, J.S., Pestronk, A., Conolly, A.M., Druley, T.E. *et al.* (2010) Myosin binding protein C1: a novel gene for autosomal dominant distal arthrogryposis type 1. *Hum. Mol. Genet.*, **19**, 1165–1173.
- Sung, S.S., Brassington, A.M., Grannatt, K., Rutherford, A., Whitby, F.G., Krakowiak, P.A., Jorde, L.B., Carey, J.C. and Bamshad, M. (2003) Mutations in genes encoding fast-twitch contractile proteins cause distal arthrogryposis syndromes. *Am. J. Hum. Genet.*, **72**, 681–690.
- Sung, S.S., Brassington, A.M., Krakowiak, P.A., Jorde, L.B. and Bamshad, M. (2003) Mutations in TNNT3 cause multiple congenital contractures: a second locus for distal arthrogryposis type 2B. *Am. J. Hum. Genet.*, **73**, 212–214.
- Ochala, J. (2008) Thin filament protein mutations associated with skeletal myopathies: defective regulation of muscle contraction. *J. Mol. Med.*, **86**, 1197–1204.
- Laing, N.G., Dye, D.E., Wallgren-Petersson, C., Richard, G., Monnier, N., Lillis, S., Winder, T.L., Lochmüller, H., Graziano, C., Mitrani-Rosenbaum, S. *et al.* (2009) Mutations and polymorphisms of the skeletal muscle α -actin gene (ACTA1). *Hum. Mutat.*, **30**, 1267–1277.
- Lawlor, M.W., Ottenheijm, C.A., Lehtokari, V.L., Cho, K., Pelin, K., Wallgren-Petersson, C., Granzier, H. and Beggs, A.H. (2011) Novel mutations in NEB cause abnormal nebulin expression and markedly

- impaired force generation in severe nemaline myopathy. *Skeletal Muscle*, **1**, 23.
12. Romero, N.B., Monnier, L., Viollet, L., Cortay, A., Chevallay, M., Leroy, J.P., Lunardi, J. and Fardeau, M. (2003) Dominant and recessive core disease associated with RYR1 mutations and fetal akinesia. *Brain*, **126**, 2341–2349.
 13. Riemersma, S., Vincent, A., Beeson, D., Newland, C., Hawke, S., Vernet-der Garabedian, B., Eymard, B. and Newsom-Davis, J. (1996) Association of arthrogryposis multiplex congenital with maternal antibodies inhibiting fetal acetylcholine receptor function. *J. Clin. Invest.*, **98**, 2538–2563.
 14. Hoffmann, K., Muller, J.S., Stricker, S., Megarbane, A., Rajab, A., Lindner, T.H., Cohen, M., Chouery, E., Adaimy, L., Ghanem, I. *et al.* (2006) Escobar syndrome is a prenatal myasthenia caused by disruption of the acetylcholine receptor fetal gamma subunit. *Am. J. Hum. Genet.*, **79**, 303–312.
 15. Morgan, N.V., Brueton, L.A., Cox, P., Grealley, M.T., Tolmie, J., Pasha, S., Aligiani, I.A., van Bokhoven, H., Marton, T., Al-Gazali, L. *et al.* (2006) Mutations in the embryonal subunit of the acetylcholine receptor (CHRN3) cause lethal and Escobar variants of multiple pterygium syndrome. *Am. J. Hum. Genet.*, **79**, 390–395.
 16. Vogt, J., Harrison, B.J., Spearman, H., Cossins, J., Vermeer, S., ten Cate, L.N., Morgan, N.V., Beeson, D. and Maher, E.R. Mutation analysis of CHRNA1, CHRNB1, CHRN3, and RAPS3 genes in multiple pterygium syndrome/fetal akinesia patients. *Am. J. Hum. Genet.*, **82**, 222–227.
 17. Brownlow, S., Webster, R., Croxson, R., Brydson, M., Neville, B., Lin, J.P., Vincent, A., Newsom-Davis, J. and Beeson, D. (2001) Acetylcholine receptor delta subunit mutations underlie a fast-channel myasthenic syndrome and arthrogryposis multiplex congenita. *J. Clin. Invest.*, **108**, 125–130.
 18. Vogt, J., Morgan, N.V., Marton, T., Maxwell, S., Harrison, B.J., Beeson, D. and Maher, E.R. (2009) Germline mutation in DOK7 associated with fetal akinesia deformation sequence. *J. Med. Genet.*, **46**, 338–340.
 19. Michalk, A., Stricker, S., Becker, J., Rupps, R., Pantzar, T., Miertus, J., Botta, G., Naretto, V.G., Janetzki, C., Yqoob, N. *et al.* (2008) Acetylcholine receptor pathway mutations explain various fetal akinesia deformation sequence disorders. *Am. J. Hum. Genet.*, **82**, 464–476.
 20. Valdenaire, O., Richards, J.G., Faull, R.L.M. and Schweizer, A. (1999) XCE, a new member of the endothelin-converting enzyme and neutral endopeptidase family, is preferentially expressed in the CNS. *Mol. Brain Res.*, **64**, 211–221.
 21. Kiryu-Seo, S., Sasaki, M., Yokohama, H., Nakagomi, S., Hirayama, T., Aoki, S., Wada, K. and Kiyama, H. (2000) Damage-induced neuronal endopeptidase (DINE) is a unique metalloproteinase expressed in response to neuronal damage and activates superoxide scavengers. *Proc. Natl Acad. Sci. USA*, **97**, 4345–4350.
 22. Zhang, Y., Luoh, S.M., Hon, L.S., Baertsch, R., Wood, W.I. and Zhang, Z. (2007) GeneHub-GEPIs: digital expression profiling for normal and cancer tissues based on an integrated gene database. *Nucleic Acids Res.*, **35**, W152–W158.
 23. Valdenaire, O., Rohrbacher, E., Langeveld, A., Schweizer, A. and Meijers, C. (2000) Organization and chromosomal localization of the human *ECE1* (XCE) gene encoding a zinc metalloproteinase involved in the nervous control of respiration. *Biochem. J.*, **346**, 611–616.
 24. Nagata, K., Kiryu-Seo, S. and Kiyama, H. (2006) Localization and ontogeny of damage-induced neuronal endopeptidase mRNA-expressing neurons in the rat nervous system. *Neuroscience*, **141**, 299–310.
 25. Oefner, C., D'Arcy, A., Hennig, M., Winkler, F.K. and Dale, G.E. (2000) Structure of human neutral endopeptidase (neprilysin) complexed with phosphoramidon. *J. Mol. Biol.*, **296**, 341–349.
 26. Oefner, C., Roques, B.P., Fournie-Zaluski, M.C. and Dale, G.E. (2004) Structural analysis of neprilysin with various specific and potent inhibitors. *Acta Crystallogr. D Biol. Crystallogr.*, **D60**, 392–396.
 27. Oefner, C., Pierau, S., Schulz, H. and Dale, G.E. (2007) Structural studies of a bifunctional inhibitor of neprilysin and DPP-IV. *Acta Crystallogr. D Biol. Crystallogr.*, **D63**, 975–981.
 28. Benoit, A., Vargas, M.A., Desgroseillers, L. and Boileau, G. (2004) Endothelin-converting enzyme-like 1 (ECE1) is present both in the plasma membrane and in the endoplasmic reticulum. *Biochem. J.*, **380**, 881–888.
 29. Mercuri, E., Rutherford, M., Barnett, A., Foglia, C., Haataja, L., Counsell, S., Cowan, S. and Dubowitz, L. (2002) MRI lesions and infants with neonatal encephalopathy: is the apgar score predictive? *Neuropediatrics*, **33**, 150–156.
 30. Farrugia, M.E., Robson, M.D., Clover, L., Anslow, P., Newsom-Davis, J., Kennett, R., Hilton-Jones, D., Matthews, P.M. and Vincent, A. (2006) MRI and clinical studies of facial and bulbar muscle involvement in MuSK antibody-associated myasthenia gravis. *Brain*, **129**, 1481–1492.
 31. Bland, N.D., Pinney, J.W., Thomas, J.E., Turner, A.J. and Isaac, R.E. (2008) Bioinformatic analysis of the neprilysin (M13) family of peptidases reveals complex evolutionary and functional relationships. *BMC Evol. Biol.*, **8**, 16.
 32. Nicholson, P., Yepiskoposyan, H., Metze, S., Zamudio Orozco, R., Kleinschmidt, N. and Mühlemann, O. (2010) Non sense-mediated mRNA decay in human cells: mechanistic insights, functions beyond quality control and the double-life of NMD factors. *Cell. Mol. Life Sci.*, **67**, 677–700.
 33. Grantham, R. (1974) Amino acid difference formula to explain protein evolution. *Science*, **185**, 862–864.
 34. MacLeod, K.J., Fuller, R.S., Scholten, J.D. and Ahn, K. (2001) Conserved cysteine and tryptophan residues of the endothelin-converting enzyme-1 CXAW motif are critical for protein maturation and enzyme activity. *J. Biol. Chem.*, **276**, 30608–30614.
 35. Dixon, P.H., Christie, P.T., Wooding, C., Trump, D., Grieff, M., Holm, I., Gertner, J.M., Schmidtke, J., Shah, B., Shaw, N. *et al.* (1998) Mutational analysis of PHEX gene in X-linked hypophosphatemia. *J. Clin. Endocrinol. Metab.*, **83**, 3615–3623.
 36. Filisetti, D., Ostermann, G., von Bredow, M., Strom, T., Filler, G., Ehrlich, J., Pannetier, S., Garnier, J.M., Rowe, P., Francis, F. *et al.* (1999) Non-random distribution of mutations in the PHEX gene, and under-detected missense mutations at non-conserved residues. *Eur. J. Hum. Genet.*, **7**, 615–619.
 37. Tyynismaa, H., Kaitila, I., Nääntö-Salonen, K., Ala-Houhala, M. and Alitalo, T. (2000) Identification of fifteen novel PHEX gene mutations in Finnish patients with hypophosphatemic rickets. *Hum. Mutat.*, **15**, 383–384.
 38. Nagata, K., Kiryu-Seo, S., Maeda, M., Yoshida, K., Morita, T. and Kiyama, H. (2010) Damage-induced neuronal endopeptidase is critical for presynaptic formation of neuromuscular junctions. *J. Neurosci.*, **30**, 6954–6962.
 39. Schweizer, A., Valdenaire, O., Köster, A., Lang, Y., Schmitt, G., Lenz, B., Bluthmann, H. and Rohrer, J. (1999) Neonatal lethality in mice deficient in XCE, a novel member of the endothelin-converting enzyme and neutral endopeptidase family. *J. Biol. Chem.*, **274**, 20450–20456.
 40. Mishina, M., Takai, T., Imoto, K., Noda, M., Takahashi, T., Numa, S., Methfessel, C. and Sakmann, B. (1986) Molecular distinction between fetal and adult forms of muscle acetylcholine receptor. *Nature*, **321**, 406–411.
 41. Hesselmans, L.F., Jennekens, F.G., Van den Oord, C.J., Veldman, H. and Vincent, A. (1993) Development of innervation of skeletal muscle fibers in man: relation to acetylcholine receptors. *Anat. Rec.*, **236**, 553–562.
 42. Rump, A., Kasper, G., Hayes, C., Wen, G., Starke, H., Liehr, T., Lehmann, R., Lagemann, D. and Rosenthal, A. (2001) Complex arrangement of genes within a 220-kb region of double-duplicated DNA on human 2q37.1. *Genomics*, **73**, 50–55.
 43. Ruschendorf, F. and Nurnberg, P. (2005) ALOHOMORA: a tool for linkage analysis using 10K SNP array data. *Bioinformatics*, **21**, 2123–2125.
 44. Abecasis, G.R., Cherny, S.S., Cookson, W.O. and Cardon, L.R. (2002) Merlin-rapid analysis of dense genetic maps using sparse gene flow trees. *Nat. Genet.*, **30**, 97–101.
 45. Jarraya, M., Quijano-Roy, S., Monnier, N., Béhin, A., Avila-Smirnov, D., Romero, N.B., Allamand, V., Richard, P., Barois, A., May, A. *et al.* (2012) Whole-Body muscle MRI in a series of patients with congenital myopathy related to TPM2 gene mutations. *Neuromuscul. Disord.*, **22**, S137–147.
 46. Bevilacqua, J.A., Monnier, N., Bitoun, M., Eymard, B., Ferreira, A., Monges, S., Lubieniecki, F., Taratuto, A.L., Laquerrière, A., Claeys, K.G. *et al.* (2011) Recessive RYR1 mutations cause unusual congenital myopathy with prominent nuclear internalization and large areas of myofibrillar disorganization. *Neuropathol Appl Neurobiol*, **37**, 271–284.
 47. Tidswell, T. and Pitt, M.C. (2007) A new analytical method to diagnose congenital myasthenia with stimulated single-fiber electromyography. *Muscle Nerve*, **35**, 107–110.